Journal of Rock Mechanics and Geotechnical Engineering. 2012, 4 (2): 149–159

Journal of Rock Mechanics and Geotechnical Engineering

Journal online: www.rockgeotech.org

Numerical simulations of kinetic formation mechanism of Tangjiashan landslide

Gang Luo[1*], Xiewen Hu[1, 2], Chengzhuang Gu[1], Ying Wang[1]

[1] Faculty of Geosciences and Environmental Engineering, Southwest Jiaotong University, Chengdu, 610031, China

[2] Aseismic Engineering Technology Key Laboratory of Sichuan Province, Southwest Jiaotong University, Chengdu, 610031, China

Received 23 March 2011; received in revised form 29 June 2011; accepted 12 January 2012

Abstract: Tangjiashan landslide is a typical high-speed landslide hosted on consequent bedding rock. The landslide was induced by Wenchuan earthquake at a medium-steep hill slope. The occurrence of Tangjiashan landslide was basically controlled by the tectonic structure, topography, stratum lithology, slope structure, seismic waves, and strike of river. Among various factors, the seismic loading with great intensity and long duration was dominant. The landslide initiation exhibited the local amplification effect of seismic waves at the rear of the slope, the dislocation effect on the fault, and the shear failure differentiating effect on the regions between the soft and the hard layers. Based on field investigations and with the employment of the distinct element numerical simulation program UDEC (universal distinct element code), the whole kinetic sliding process of Tangjiashan landslide was represented and the formation mechanism of the consequent rock landslide under seismic loading was studied. The results are helpful for understanding seismic dynamic responses of consequent bedding rock slopes, where the slope stability could be governed by earthquakes.

Key words: Tangjiashan high-speed landslide; formation mechanism; sliding process; numerical simulations

1 Introduction

The 2008 Wenchuan earthquake is one of the major natural disasters in China and caused serious casualties, enormous property losses, and further earthquake-induced disasters (Stone, 2008; Xiao et al., 2010). Among them, the Tangjiashan Barrier Lake is the largest potential hazard formed by a large consequent bedding rock landslide to block the Tongkou River in Beichuan County. At present, a lot of fruitful results for landslide-barrier lakes have been achieved. For example, Cheng et al. (2008), Ma and Luo (2008) and Hu et al. (2009) analyzed the mechanism of Tangjiashan landslide and breaking mode of its barrier dam. They presented many triggering factors of landslide by empirical knowledge. But detailed effects of various factors on the landslide were not fully interpreted. Wang et al. (2009) used the finite element method (FEM) to simulate tensile fracturing process of slopes with a single weak plane under strong earthquakes. Feng et al. (2009) conducted finite element numerical analysis and adopted shaking table to simulate the earthquake-induced mechanism of single- and double-side slopes. Sun et al. (2010) proposed that earthquake-induced liquefaction occurring on the potential sliding surface played an important role in generating the rapid and long run-out landslide. Yang et al. (2009) carried out numerical simulations of particle flow on the loose slopes' landslide under seismic loading. Xu and Huang (2008) presented kinetic characteristics of cracking, horizontal throwing and debris flows triggered by earthquake. Huang et al. (2008) elaborated the basic characteristics and formation mechanism of large-scale landslide at Daguangbao.

Most of the numerical methods used in the above researches are roughly based on finite elements or FEM, in which the slope is assumed to be a continuum. However, these methods are often subjected to small deformation assumption and do not consider the vital role of joints in rock slopes. The failure of rock slopes

Doi: 10.3724/SP.J.1235.2012.00149

*Corresponding author. Tel: +86-13882206250; E-mail: exqqduck@126.com

Supported by the National Natural Science Foundation of China (40772175, 40972175), the Scientific Research Fund of Southwest Jiaotong University (2008–A01), the Doctoral Student Innovation Fund of Southwest Jiaotong University, and the National Natural Science Foundation of China-Yunan Joint Fund (U1033601)

is typically controlled by joints and interfaces, thus the modeling of these discontinuities is crucial to understand the mechanism of slope failure and kinetic responses of landslides. Fortunately, discrete element methods (DEMs) can address the deficiencies in solving discontinuous rock masses by finite elements and FEM (Bardet and Scott, 1985). Taking the Tangjiashan slope as an example, the formation mechanism of consequent bedding rock landslide and the kinetic movement process under earthquake are analyzed using the discrete element software UDEC (Itasca, 1999) in this paper.

2 Geological setting of Tangjiashan landslide

Tangjiashan high-speed landslide is regionally located between Longmenshan central fault (Beichuan—Yingxiu fault) and Longmenshan rear fault. The distance from Tangjiashan to the Beichuan—Yingxiu fault is approximately 2.3 km (Fig. 1).

The occurrence of Tangjiashan landslide was controlled by various factors. Therefore, a comprehensive analysis should be conducted to provide an early-warning prediction of landslide in the vicinity of earthquake-prone areas. As for Tangjiashan landslide itself, its formation can mainly be analyzed from the following three aspects.

2.1 Effects of seismic wave propagation

Tangjiashan is located at the north of Longmenshan central fault on the hanging wall. The statistics of the distance between the causative fault and the corresponding earthquake-hit disaster areas show that more than 70% of geohazards are basically developed at the hanging wall within 3 km away from rupture (Xu et al., 2009). In addition, both the spatial distribution and the sliding direction of Tangjiashan landslide have a close relationship with the direction of seismic wave propagation, exhibiting a local amplification effect of seismic waves at the rear of the slope and the dislocation effect of the fault.

The local amplification effect of seismic waves at the rear of the slope means that the landslide density at the rear of the slope is higher than that at the front side, almost perpendicular to the triggering seismic fault (Fig. 2), which is related to seismic wave propagation direction in the valley. The dislocation effect of the fault shows that the sliding and movement directions of most regional landslides are basically perpendicular to the triggering seismic fault.

2.2 Topography

More than 90% of barrier lakes are related to high-speed landslides induced by earthquake (Schuster and Costa, 1986; Costa and Schuster, 1988; Asansa et al., 1991; Brooks and Hickin, 1991; Jennings et al., 1991; Perrin and Hancox, 1991; Picard, 1991; Mora et al., 1993). It is observed that the toe of surface of rupture is above or slightly below the riverbed accumulation, which has a negative effect on prevention of the landslide body from sliding. This will cause the landslide to ultimately block the river. Therefore, a river-blocking landslide needs specific topography and geo-morphology, such as cutting depth of river valleys and lateral ditches, slope gradient, valley width, stream flow, large volume of landslides body and so on (Chai et al., 1996).

(1) The deeper cutting depth of river valleys and lateral ditches mean that the gravitational energy of soils and rocks is greater. It is negative to slope stability. Once the failure of slopes at the deeper

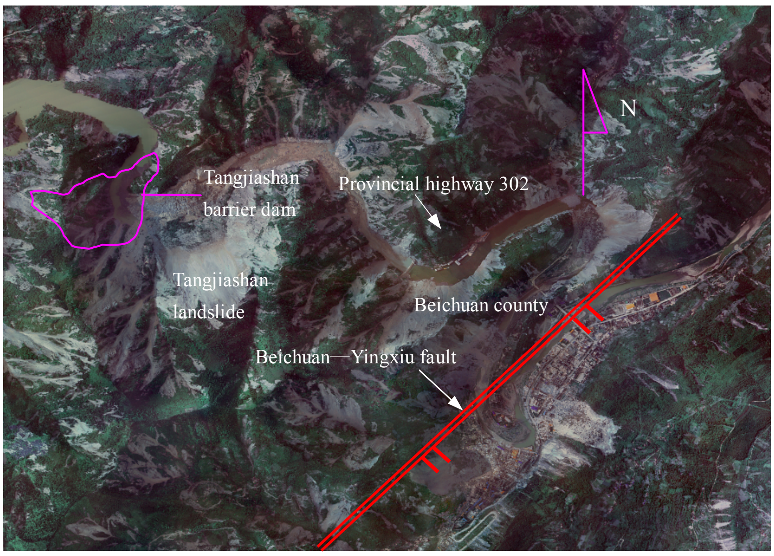

Fig. 1 Location of Beichuan—Tangjiashan barrier dam and Beichuan—Yingxiu fault.

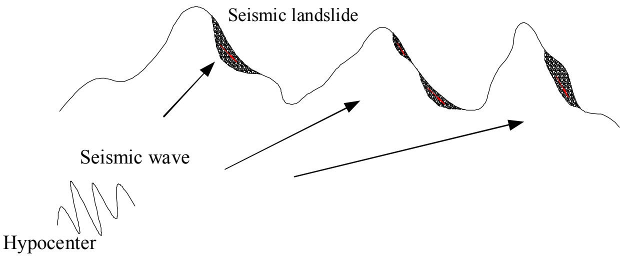

Fig. 2 Easily induced landslide at the rear of slope relative to seismic wave propagation direction.

valleys occurs, high-momentum landslide will have a strong impact on the riverbed, and finally it will climb to a certain height over the opposite bank, resulting in complete blockage of the river.

(2) Whether the slopes are steep or gentle, bedding planes have a direct influence on the stability of the rock slopes. In a global sense, because of a long-term weathering history and gravity-induced failures of the surface layers, it is more likely to develop landslides on the consequently layered slopes than that on the oblique-reversely layered ones. Thus, a shear sliding surface is easier to form along the bedding planes.

Before earthquake, the terrain gradient of Tangjiashan slope was about 40°, the slope toe's elevation was about 665 m, and the crest watershed's elevation was nearly 1 500 m (Fig. 3). The height difference is up to 835 m, thus the geopotential gravitational energy is large. Moreover, the deep cutting valleys and the large and small ditches in the terrain will cause Tangjiashan to form three free faces, providing an effective way for high-speed mass to slide. Meanwhile, Tangjiashan slope is located at the concave bank of the Tongkou River. Due to the long-term erosion of riverbank on the toe of the slope, its lower accumulation of riverbed is considerably thin. The river surface width is 100–130 m and water depth is less than 4 m. As the river flows slowly, the volume of the landslide sliding into the river reaches 20.37×10^6 m^3. Because the hydro-dynamic force was far less than the frictional force at the bottom of the barrier dam, the dam body completely blocked the river and made the upstream river rise continually. Clearly, these topographical features are the favorable conditions for river-blocking formation of Tangjiashan landslide.

2.3 Different effects of shear failure on soft and hard layers

The bedrock of Tangjiashan slope consists of hard siliceous rocks and soft marlstone rocks of Qingping group of lower Cambrian system ($\in_{1c}$). Due to the differences of modulus and stiffness of interfaces between soft and hard rock layers, the rapid deformation and the progressive shear failure under seismic loading were observed on the soft rock layers.

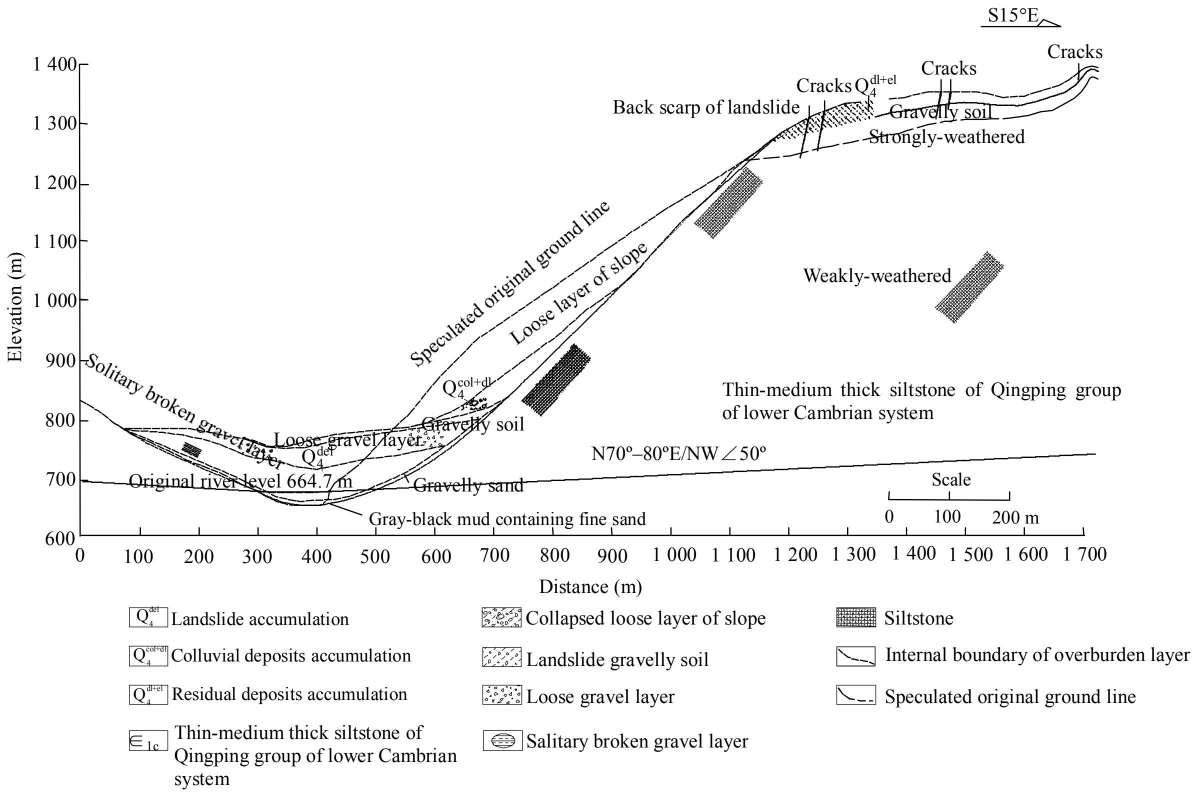

Fig. 3 Engineering geological longitudinal section of Tangjiashan landslide and its barrier dam.

Meanwhile, the interfaces were also stretched and distorted with rapidly decreasing shear strength. Thus, a slip surface was formed along the interfaces or the soft rock layers (Luo et al., 2010). On the contrary, the hard rock layers showed elastoplastic deformation under earthquake. This is the reason that after sliding, Tangjiashan barrier dam has quasi-layer-structure rock masses, which still maintains a relatively intact integrity.

The strata attitude of Tangjiashan bedrock is N60ºE/NW∠60º, displaying the consequent slope on the right bank. So this steeply dipping consequent structure is another factor to cause the instability of Tangjiashan landside under earthquake.

3 Kinetic analysis

The general UDEC is suitable for processing discontinuous media. It allows for the occurrence of discrete blocks translation, rotation, or even complete separation. Also, it can automatically identify newly generated interfaces in practical calculation. Thus, UDEC can be used to study the progressive failure of rock slopes and to evaluate the impact of joints, faults, and bedding planes.

Based on peak ground acceleration (PGA) records of Wenchuan earthquake (Figs. 4 and 5), in which the Tangjiashan site's PGA is 287–547 gal (1 gal = 1×10^{-2} m/s^2). A modified input acceleration time-history curve can be obtained after baseline correction by lowpass filtering to suppress frequencies that are higher than 10 Hz (Fig. 6), in which the duration is 60 s and Arias intensity is grade XI. In this model, the power spectrum is computed by means of fast Fourier transformation (FFT) of the input time-history (Fig. 7). The acceleration-frequency power spectrum displays the statistical property frequency of the input ground motion. In Longmenshan area, earthquake-induced landslides hazards are more serious in the locations where PGA is greater than 0.2 g (Wang et al., 2010). The maximum input time-history is 0.547 g, hence the input time-history can give a relatively true simulation of the deformation and failure of Tangjiashan slope and the movement process of the landslide.

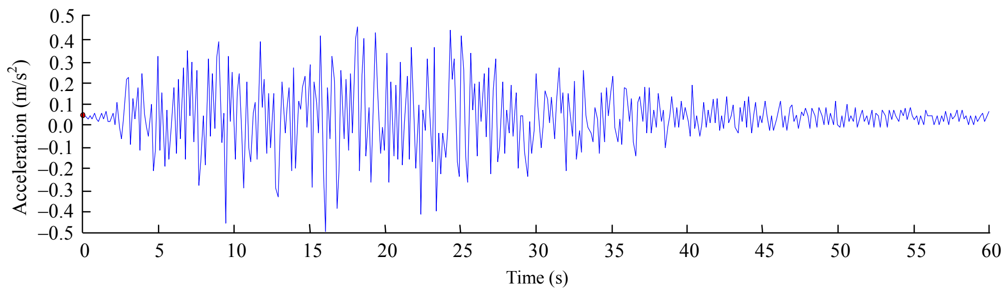

Fig. 4 Peak acceleration record of Wenchuan earthquake (according to the China Seismological Bureau).

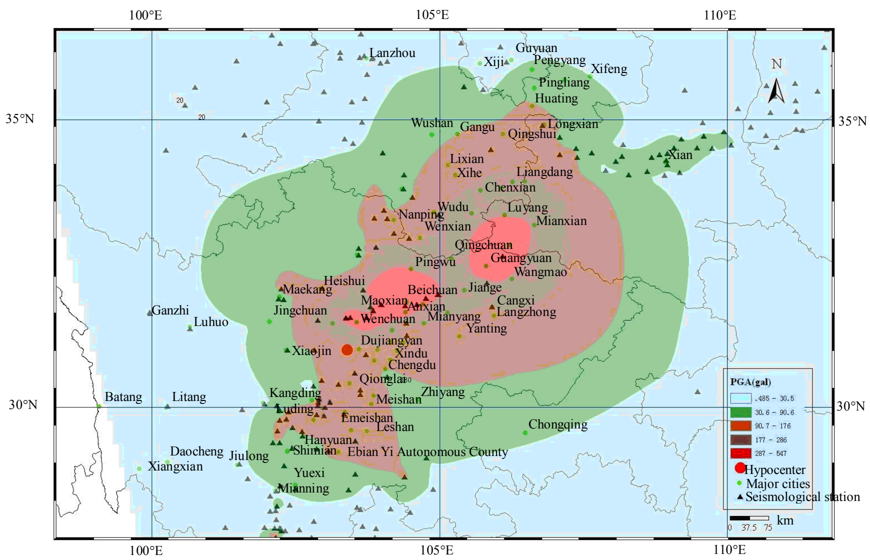

Fig. 5 Distribution of PGA from the main shock (according to the China Seismological Bureau).

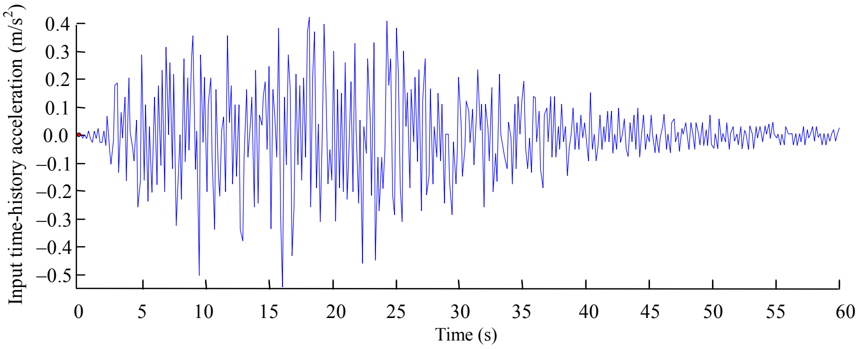

Fig. 6 Time-history curve input in numerical model.

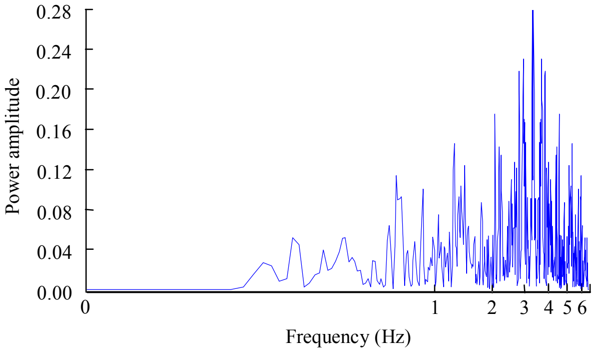

Fig. 7 Acceleration-frequency power spectrum curve of filtering at 10 Hz.

3.1 UDEC numerical model

The longitudinal section in Fig. 3 is taken as the prototype in the numerical model (Fig. 8).

Six monitoring points numbered from 1 to 6 have been set up in the landslide body to monitor the velocity time-history curves of Tangjiashan landslide induced by the earthquake. In the model, the landslide units are composed of strongly weathered rock masses. And the bedrock is composed of weakly weathered ones. The structural planes are mainly joints and bedding planes. The physico-mechanical parameters of rock masses and structural planes, according to experimental parameters of barrier dam materials and the results (Wu et al., 2008; Hu et al., 2009; Cui et al., 2010), are shown in Tables 1 and 2, respectively.

As the normal and tangential stiffnesses (K_n and K_s) cannot be determined in field, a value of 10 times that of the hardest adjacent region is taken according to the UDEC manual, namely

$$K_n = K_s \le 10\left[\max\left(\frac{K + 4G/3}{\Delta z_{min}}\right)\right] \tag{1}$$

where K is the bulk modulus, G is the shear modulus, and Δz_{min} is the minimum size of a continuous domain in normal direction between joint planes (Itasca, 1999).

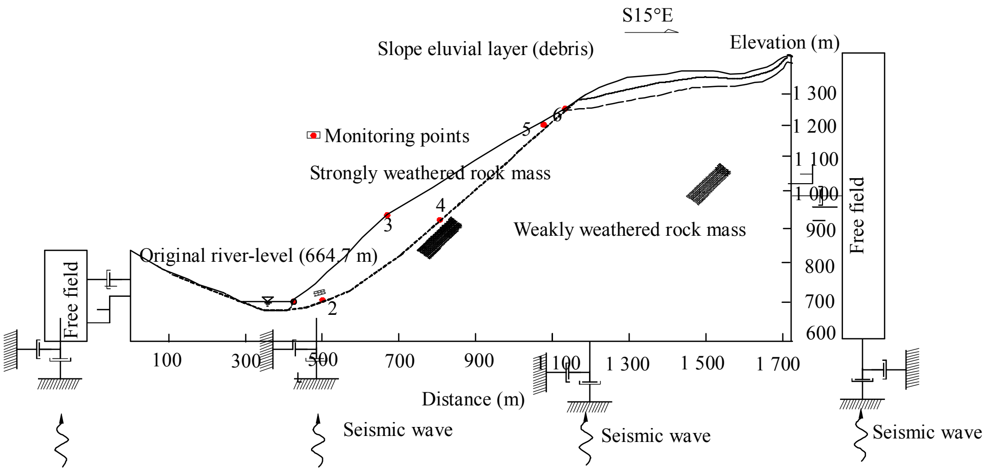

Fig. 8 Distribution of monitoring points in numerical model of Tangjiashan landslide.

Table 1 Physico-mechanical parameters of rock masses.

Rock mass	Natural density (kg/m^3)	Cohesion (MPa)	Internal friction angle (°)	Bulk modulus (GPa)	Shear modulus (GPa)
Slope eluvial layer (debris)	2 000	0.03	35	1.3	0.8
Strongly weathered rock masses	2 550	0.12	30	1.2	0.8
Weakly weathered rock masses	2 650	0.82	42	2	1.2

Table 2 Mechanical parameters of structural planes.

Structural plane	Normal stiffness (GPa/m)	Shear stiffness (GPa/m)	Internal friction angle (°)	Cohesion (MPa)	Tensile strength (MPa)
Bedding plane	3.6	1.2	30	0.5	0.05
Joint plane	3.6	1.2	23	0.3	0.03

3.2 Numerical constitutive model and boundary conditions

In this model, the strata dip angle is taken as 50°. Due to the calculation time limit and the accuracy requirements, the spacing of joints is taken as 10 m and the grid is divided into 139 703 discrete triangular elements. The rock materials treated by plain-strain contain three layers, namely, a slope eluvial layer (debris), a strongly weathered rock layer and a weakly weathered rock layer (Fig. 9). All of them are adopted in the perfect plastic model, while the yield criterion adopts the Mohr-Coulomb failure criterion. Moreover, a Coulomb-slip model is used for bedding planes and joint planes with surface contact. The model uses the viscous boundary and the local damping that is frequency-independent, and no estimation of the natural frequency of the modeled system is needed. The free-field boundaries are adopted for the lateral grids of bedrock domain to eliminate the radiation damping effect. When the static equilibrium under gravity load is obtained, the dynamic calculation begins under the excitation of seismic wave input from the model bottom.

The local damping coefficient can be written as

$$\alpha_{\mathrm{L}} = \pi d \tag{2}$$

where α_{L} is the local damping coefficient, and d is the damping coefficient. Thus, the use of local damping is simpler than Rayleigh damping, since the frequency needs no specifying. Referring to the user's manual of UDEC (Itasca, 1999), the damping coefficient d could be set to 0.05, so the local damping coefficient α_{L} is 0.157. Energy is dissipated in the forms of joints' slip and separation during dynamic loading, and it tends to make the selection of damping parameters less critical to the outcome of the analysis.

3.3 Seismic loading input

When the acceleration table is applied to the bottom boundary of the model, it is suggested that the size of mesh generation should be controlled by the shortest wavelength of input fluctuation (Itasca, 1999). Thus the maximum size of the grid can be set as Δl and the shortest wavelength of seismic wave λ, and Δl should be less than $(1/10-1/8)\lambda$. The highest frequency of the input wave $f_{\max}$, which cannot make waveform distorted, can be written as

$$\left.\begin{aligned} f_{\max} &= \frac{c}{\lambda} = \frac{c_{\mathrm{S}}}{10\Delta l} \\ c_{\mathrm{S}} &= \sqrt{G/\rho} \end{aligned}\right\} \tag{3}$$

where ρ is the medium density (kg/m^3), c_{S} is the S-wave velocity of the medium (m/s).

In Eq. (3), the mesh size of this model can be determined, allowing for the maximum input frequency of 14 Hz. The maximum input frequency of the dynamic load is 6.6 Hz. Therefore, in the simulation, the selected grid size of the discrete elements can properly meet those requirements.

3.4 Stress analysis of natural slope

As observed in Fig. 10, the σ_{xx} and σ_{yy} contours of the slope are smooth in the natural state, transferring uniformly from the bottom to the crest and rarely

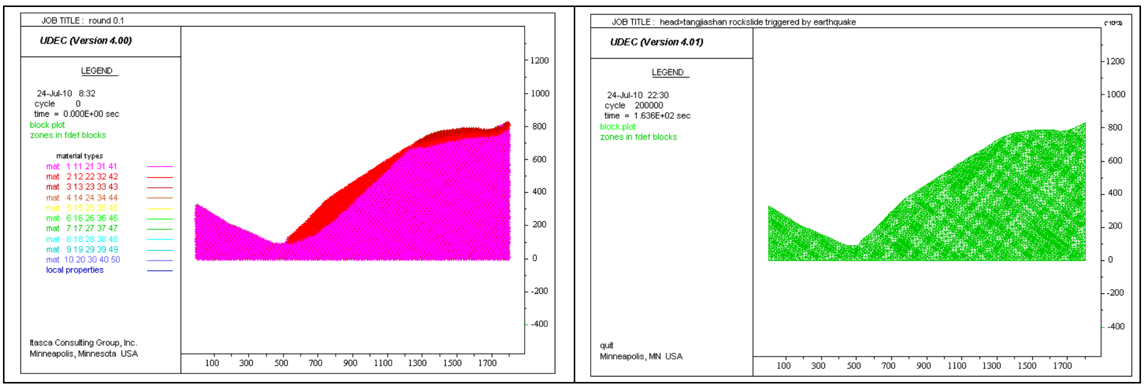

Fig. 9 Stratified material and calculation mesh of Tangjiashan landslide.

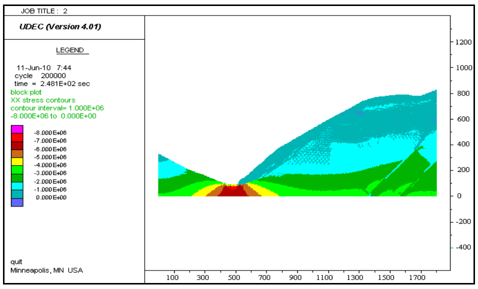

(a) σ_{xx} stress contour (Pa).

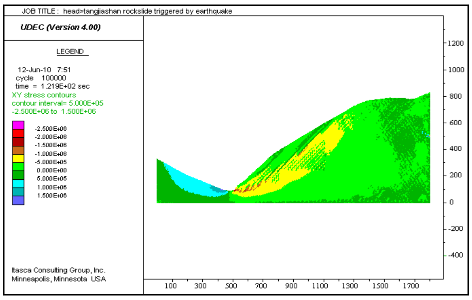

(b) σ_{xy} stress contour (Pa).

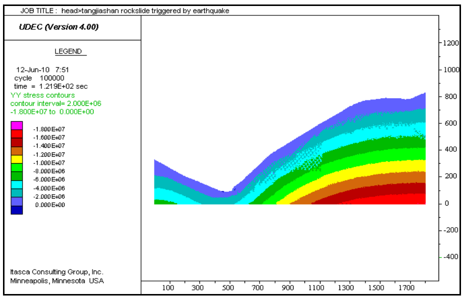

(c) σ_{yy} stress contour (Pa).

Fig. 10 Stress contours of slope in nature condition.

having intercross. The value of σ_{xx} ranges from 0 to 5 MPa and σ_{yy} ranges from 0 to 14 MPa, illustrating that the whole slope is in a homogeneous compression state. Simultaneously, σ_{xy} is concentrated on the toe of slope with the maximum shear stress of 1.5 MPa, showing that only the toe of slope is in shear state. The above numerical results conform to the classical theory, indicating the stability of the slope.

3.5 Simulations of landslide under seismic loading

As shown in Figs. 11 and 12, during the first 25 s of strong shaking, the shallow and the posterior parts of landslide started to slide at a slow rate due to the resistance of the lockup section from oblique layers at the toe of the slope. During the following period of 25–35 s, after the lockup section was broken, the landslide as a unit moved and slid at a substantially high rate. During the follow-up period of 35–45 s, the landslide clasped and climbed upward to the opposite bank. Its front part was retarded, whereas its posterior part still remained at a high-speed sliding downwards, and the sliding velocity rate gradually slowed down. After 45 s, the landslide came to a full stop and blocked the river, thus a barrier dam was formed. According to a witness at the site, it is said that the landslide process lasted for about half a minute. By comparing the terrain from numerical results and the one from detailed geological investigations of the barrier dam, it can be seen that the terrain is basically the same. These above two evidences verify the numerical results.

In total, the mechanism of the landslide-induced barrier lake can be summarized as follows: (1) there were shearing surfaces in the forefront edge of the consequent slope, which was caused by earthquake and tension crack in the posterior edge; (2) the riverbed was ploughed by landslide forward edge, and the thither slope was uplifted for inhibition; (3) the back edge of the landslide stood and glided; and (4) finally, it dammed and blocked the river.

3.6 Formation mechanism of earthquake-induced landslide

When a consequent slope with a medium-high dip angle suffered a powerful earthquake, tensile failure along weak planes was generated on the upper

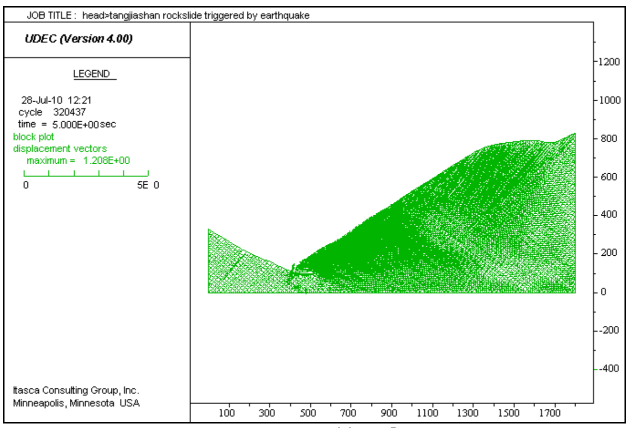

(a) t = 5 s.

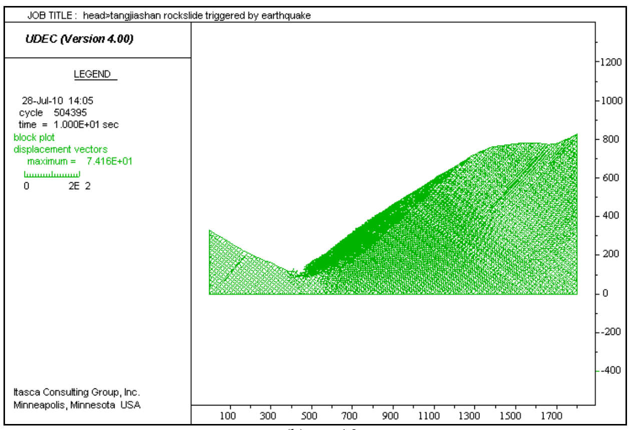

(b) t = 10 s.

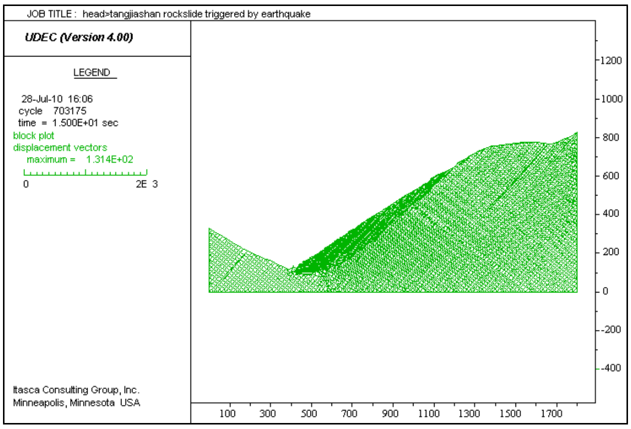

(c) $t = 15$ s.

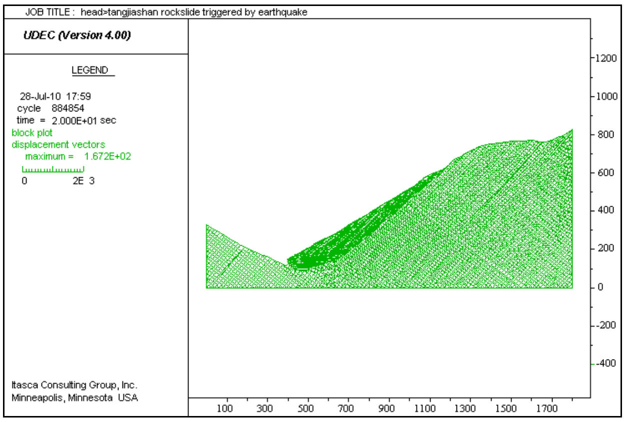

(d) $t = 20$ s.

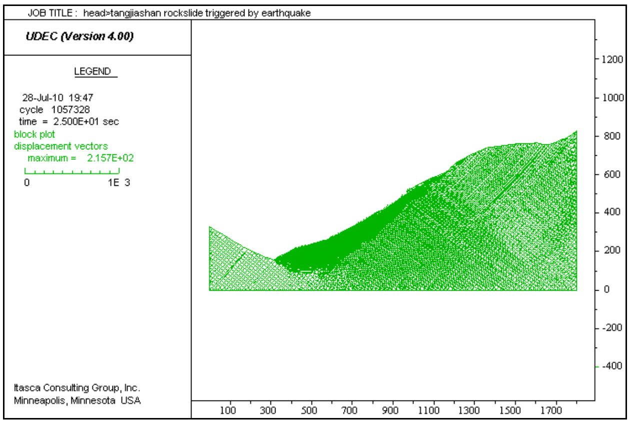

(e) $t = 25$ s.

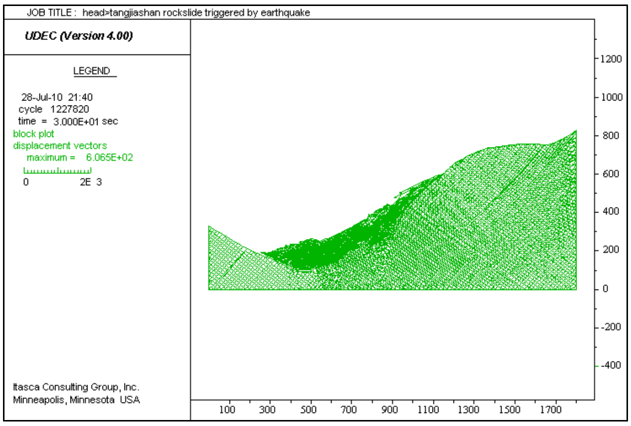

(f) $t = 30$ s.

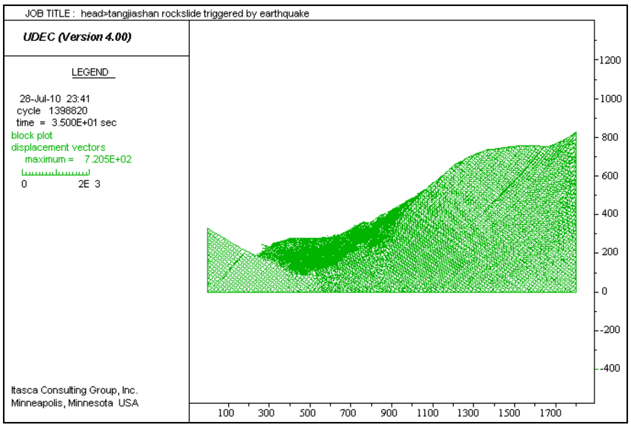

(g) $t = 35$ s.

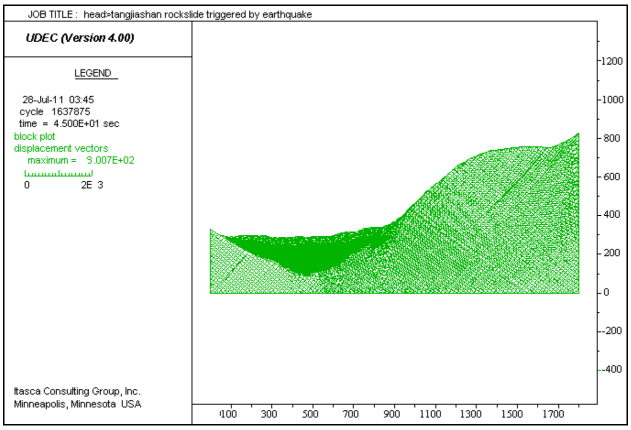

(h) $t = 45$ s.

Fig. 11 The maximum displacement vectors of units corresponding to different running times (unit: mm).

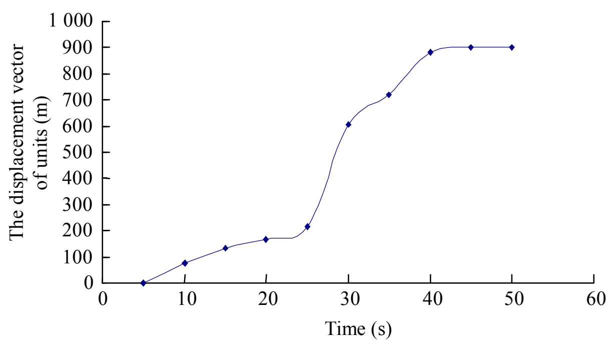

Fig. 12 Curve of the maximum displacement vector of units corresponding to different running times.

position of a slope firstly (such as bedding planes, interfaces between soft and hard rock layers, the weak interlayers, etc.). Consequently, under the continuous strong shaking, the landslide body slid at a high speed, along the tensile failure crack and the bedding plane. Eventually, the powerful driving forces of the earthquake made the oblique layer shear broken at the toe of the slope, and the tension-bedding sliding type was formed, as shown in Fig. 13.

Numerical results also show that the Tangjiashan landslide will occur after 25 s when the seismic

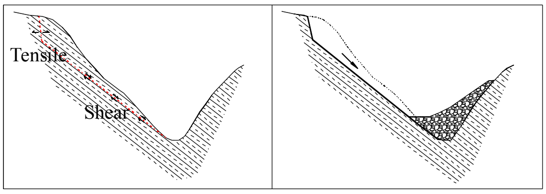

Fig. 13 Sketch of low-position bedding landslide running up to opposite side under strong earthquakes.

time-history of load is input. In order to explore the formation mechanism of Tangjiashan landslide, the progressive accumulation of shear strain and the expansion way of joint in the first 25 s are needed.

It can be observed from Figs. 14 and 15 that with continuous shaking, the shear strain simultaneously appeared at the crest and the toe of the slope, and then it rapidly propagated from the crest to the toe along the interface between the strongly and the weakly weathered rock masses, but the shear strain at the toe propagated at a relatively slow speed. With further development of shear strain and the slip surface formed, a high-speed landslide occurred along the entire slope. The above numerical results are consistent with the classical theory of consequent landslides with a medium-steep dip angle under strong earthquakes.

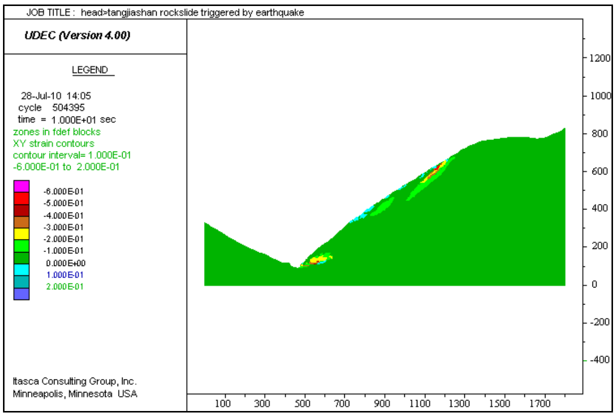

(a) t = 10 s.

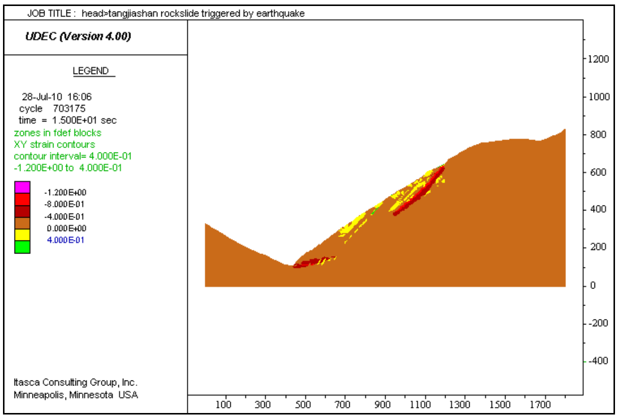

(b) t = 15 s.

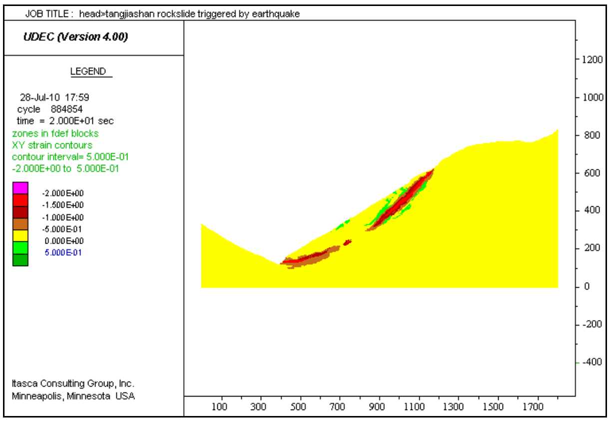

(c) t = 20 s.

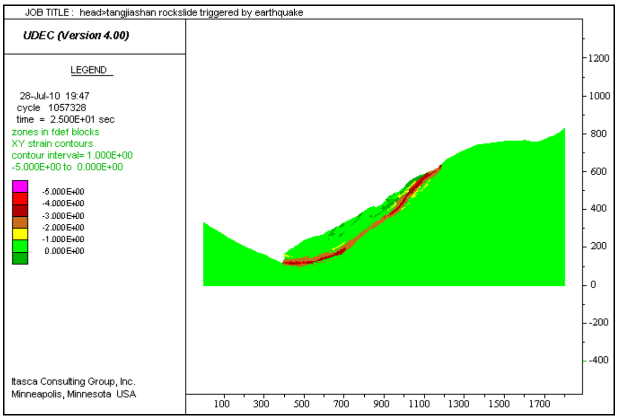

(d) t = 25 s.

Fig. 14 Shear strain contours with time under seismic loading.

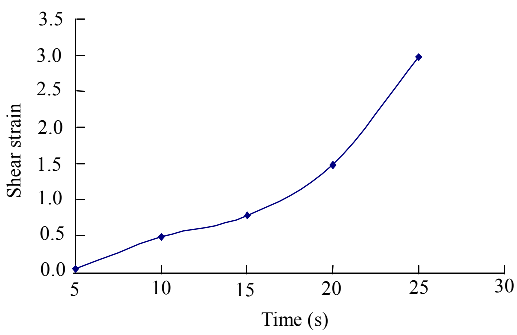

Fig. 15 Time-history curve of shear strain in sliding zone.

3.7 Velocities of monitoring points

Currently, it is regarded that the average velocity of high-speed landslides is 20 m/s or above (Cheng et al., 2007). In terms of the velocity time-histories of monitoring points, the maximum horizontal velocity of the landslide body reaches 23 m/s and the maximum vertical velocity reaches 16 m/s (Fig. 16). Therefore, Tangjiashan landslide should be categorized as a high-speed landslide.

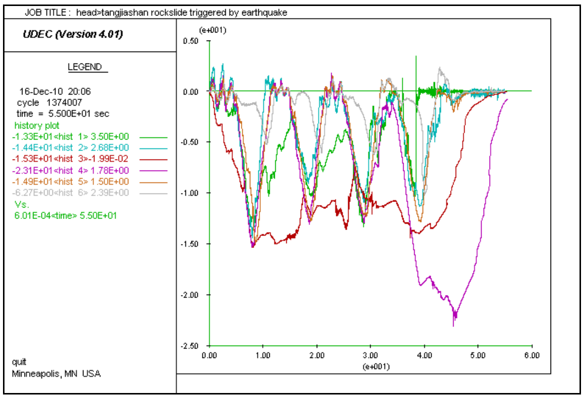

(a) Horizontal velocity time-histories.

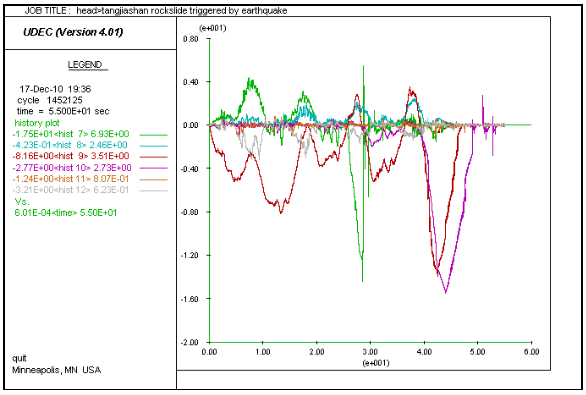

(b) Vertical velocity time-histories.

Fig. 16 Horizontal and vertical velocity time-histories of monitoring points.

4 Parametric study

According to the above analysis results, the sliding surface of Tangjiashan slope is mainly along the bedding planes, thus the parameters of the bedding plane can have a strong impact on the stability of the slope. To carry out the analysis of parametric study, the stability coefficient with different internal friction angles and cohesions of the bedding plane under natural and earthquake conditions is analyzed. The variation laws of the stability coefficient with different parameters are described in Fig. 17.

In Fig. 17(a), it is observed that under natural state, if the internal friction angle increases from 25° to 50°, provided that other conditions remain unchanged, and the stability coefficient of slope increases from 0.83 to 1.93; while under seismic loading, the stability coefficient of slope increases from 0.65 to 1.22. As seen in Fig. 17(b), under natural or seismic loading, the stability coefficient of slope increases slowly with the growth of the cohesion.

It is clear that the internal friction angle of bedding planes has a stronger impact on the stability of consequent bedding slopes than cohesion.

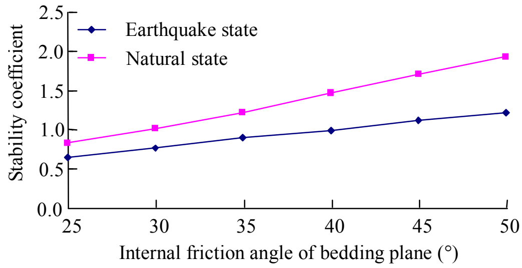

(a) Stability coefficient vs. internal friction angle.

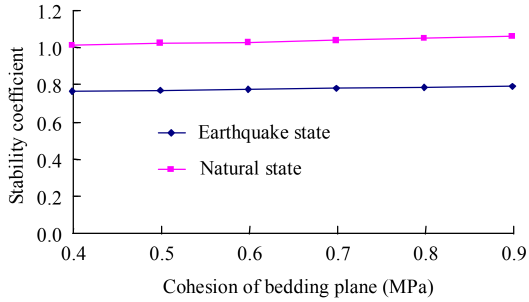

(b) Stability coefficient vs. cohesion.

Fig. 17 Variation of the stability coefficient with different internal friction angles and cohesions of bedding plane.

5 Conclusions

Based on the analysis results of Tangjiashan landslide, the following conclusions can be drawn:

(1) Among the various factors controlling Tangjiashan landslide, the intensive seismic loading and long duration are the most prominent. In addition, the features of Tangjiashan landslide exhibit: (i) the local amplification effect of seismic waves at the rear of the slope, (ii) the dislocation effect of the fault, and (iii) the shear failure differentiating effect between soft and hard layers.

(2) Through numerical simulations, the formation mechanism of Tangjiashan consequent landslide under strong earthquake is reproduced. With continuous earthquake shaking, shear strain simultaneously appeared at the crest and the toe of the slope, and then it rapidly propagated from the crest to the toe along the interfaces between strongly and weakly weathered rock masses, but the propagation of the shear strain at the toe remained at a relatively slow speed. With further development of shear strain and the formed slip surface, a high-speed landslide occurred.

(3) Based on the detailed geological investigation carried out on the location of the barrier dam and the combination of early information before the earthquake, the process of the river-blocking and the mechanism of the landslide can be summarized as follows: (i) there were shearing surfaces at the forward

edge of the consequent bedding slope, which was caused by earthquake and open tensile crack at the rear edge; (ii) the riverbed was ploughed by its forward edge, and the thither slope was uplifted for inhibition; (iii) the rear edge of the landslide slumped and slid; and (iv) finally it blocked the river to form a barrier dam.

(4) The internal friction angle of bedding planes has a more important impact on the stability of consequent bedding slopes than cohesion.

References

Asansa M, Nieto G P, Yepes H. Landslide blockage of the Pisque River, Northern Ecuador. Landslide News, 1991, 54 (1): 1 899–1 934.

Bardet J P, Scott R F. Seismic stability of fracture rock masses with the distinct element method. In: Proceedings of the 26th U.S. Symposium on Rock Mechanics (USRMS). Rotterdam: A. A. Balkema, 1985: 139–149.

Brooks G R, Hickin E J. Debris-avalanches impoundments of Squamish River Mount Caylaey area, Southwestern British Cohembia. Canadian of Earth Science, 1991, 91 (2): 129–140.

Chai Hejun, Liu Hanchao, Zhang Zhuoyuan. The main conditions of landslide dam. Journal of Geological Hazards and Environment Preservation, 1996, 7 (1): 41–46 (in Chinese).

Cheng Genwei, Wang Xiaodan, He Xiubin, Fan Jihui, Fan Jianrong. Outburst risk of barrier lakes in Sichuan, China. Journal of Mountain Science, 2008, 5 (3): 189–193.

Cheng Qiangong, Zhang Zhuoyuan, Huang Ruiqiu. Study on dynamics of rock avalanches: state of the art report. Journal of Mountain Science, 2007, 25 (1): 72–84 (in Chinese).

Costa J E, Schuster R L. The formation and failure of natural dams. Geological Society of America Bulletin, 1988, 100 (7): 1 054–1 068.

Cui Fangpeng, Hu Ruilin, Yin Yueping, Xu Qiang, Zhang Ming. Discrete element analysis of collapsing and sliding response of slope triggered by time difference coupling effects of P and S seismic waves—taking Tangjiashan landslide in Beichuan County for example. Chinese Journal of Rock Mechanics and Engineering, 2010, 29 (2): 319–327 (in Chinese).

Feng Wenkai, Xu Qiang, Huang Runqiu. Preliminary study on mechanical mechanism of slope earthquake-induced deformation. Chinese Journal of Rock Mechanics and Engineering, 2009, 28 (Supp.1): 3 124–3 130 (in Chinese).

Hu Xiewen, Huang Runqiu, Shi Yubing, Lu Xiaoping, Zhu haiyong, Wang Xuerui. Analysis of blocking river mechanism of Tangjiashan landslide and dam-breaking mode of its barrier dam. Chinese Journal of Rock Mechanics and Engineering, 2009, 28 (1): 181–189 (in Chinese).

Hu Xiewen, Luo Gang, Huang Runqiu, Zheng Yong, Lu Xiaoping, Wang Xuerui, Chen Shiyong, Shi Yubing. Study on the stability of remnant mountain body in the back scarp of Tangjiashan landslide after 5.12 Wenchuan earthquake. Chinese Journal of Rock Mechanics and Engineering, 2009, 28 (11): 2 349–2 359 (in Chinese).

Huang Runqiu, Pei Xiangjun, Li Tianbin. Basic characteristics and formation mechanism of the largest scale landslide at Daguangbao occurred during the Wenchuan earthquake. Journal of Engineering Geology, 2008, 16 (6): 730–741 (in Chinese).

Itasca Consulting Group Inc. Universal distinct element code user's manual. Minneapolis, USA: Itasca Consulting Group Inc., 1999.

Jennings D A, Webby M G, Partin D T. Tunawaea landslide dam, King Country, New Zealand. Landslide, 1991, 23 (4): 1 448–1 452.

Luo Gang, Hu Xiewen, Zhang Yao. Seismic dynamic response analysis of plane sliding rock slopes. Journal of Southwest Jiaotong University, 2010, 45 (4): 521–526 (in Chinese).

Ma Guisheng, Luo Xiaojie. Formation mechanism and engineering geologic characteristics of Tangjiashan barrier lake dam. Yangtze River, 2008, 39 (22): 46–47 (in Chinese).

Mora S, Madrigal C, Estrada J, Schuster R L. The 1992 Rio-Toro landslide Dam, Costa Rica Landslides section. [S.l.]: Disaster Prevention Research Institute, 1993: 1 183–1 128.

Perrin N D, Hancox G T. Landslide-dammed lakes in New Zealand—preliminary studies on their distribution causes and effects. In: Proceedings of the 6th International Symposium on Landslides. [S.l.]: [s.n.], 1991: 1 457–1 465.

Picard M D. Cannon landslide dam, the Abruzzi, East-Central Italy. Journal of Geological Education, 1991, 39 (5): 428–431.

Schuster R L, Costa J E. Effects of landslide damming on hydroelectric projects. In: Proceedings of the 5th International Association of Engineering Geology. [S.l.]: [s.n.], 1986: 1 295–1 307.

Stone R. Landslides, flooding pose threats as experts survey quake's impact. Science, 2008, 320: 996–997.

Sun Ping, Wang Fawu, Yin Yueping, Wang Fawu, Chen Liwei. An experimental study on the mechanism of rapid and long run-out landslide triggered by Wenchuan earthquake. Seismology and Geology, 2010, 32 (1): 98–106 (in Chinese).

Wang Laigui, Zhao Na, Li Tianbin. Finite element simulation of collapse and sliding of slope with single weak plane induced by strong earthquake. Chinese Journal of Rock Mechanics and Engineering, 2009, 28 (Supp.1): 3 163–3 167 (in Chinese).

Wang Xiuying, Nie Gaozhong, Wang Dengwei. Research on relationship between landslides and peak ground accelerations induced by Wenchuan earthquake. Chinese Journal of Rock Mechanics and Engineering, 2010, 29 (1): 82–89 (in Chinese).

Wu Aiqing, Lin Shaozhong, Ma Guisheng, Lu Bo, Zhang Lian. DDA simulation research for formation mechanism of Tangjiashan Barrier Lake. Yangtze River, 2008, 39 (22): 91–95 (in Chinese).

Xiao Shiguo, Feng Wenkai, Zhang Jianjing. Analysis of the effects of slope geometry on the dynamic response of a near-field mountain from the Wenchuan Earthquake. Journal of Mountain Science, 2010, 7 (4): 353–360.

Xu Qiang, Huang Runqiu. Kinetics characteristics of large landslides triggered by May 12th Wenchuan earthquake. Journal of Engineering Geology, 2008, 16 (6): 721–729 (in Chinese).

Xu Qiang, Pei Xiangjun, Huang Runqiu. Large-scale landslides Induced by Wenchuan earthquake. Beijing: Science Press, 2009: 7–35 (in Chinese).

Yang Qinghua, Yao Lingkan, Yang Ming. Particle flow numerical simulation of landslip of loose slope under seismic loading. Journal of Southwest Jiaotong University, 2009, 44 (4): 580–584 (in Chinese).

Zhang Chuhan, Pekau O A, Jin Feng. Application of distinct element method in dynamic analysis of high rock slopes and blocky structures. Soil Dynamics and Earthquake Engineering, 1997, 16 (6): 385–394 (in Chinese).